Effect of the Interfacial Transition Zone on the Conductivity of Portland Cement Mortars

by

Edward J. Garboczi and Dale P. Bentz
Building and Fire Research Laboratory
National Institute of Standards and Technology
Gaithersburg, MD 20899 USA

and

John D. Shane, Thomas O. Mason, and Hamlin M. Jennings
Department of Materials Science and Engineering
Northwestern University
Evanston, IL 60208 USA

Reprinted from the Journal of the American Ceramic Society, Vol. 83, No. 5, 1137-1144, 2000.

NIST
National Institute of Standards and Technology
Technology Administration, U.S. Department of Commerce

journal

J. Am. Ceram. Soc., 83 [5] 1137–44 (2000)

Effect of the Interfacial Transition Zone on the Conductivity of Portland Cement Mortars

John D. Shane,* Thomas O. Mason,* and Hamlin M. Jennings*

Department of Materials Science and Engineering, Northwestern University, Evanston, Illinois 60208-3108

Edward J. Garboczi* and Dale P. Bentz*

Building Materials Division, National Institute of Standards and Technology, Gaithersburg, Maryland 20899

The electrical conductivity of portland cement mortars was determined experimentally as a function of the volume fraction of sand and the degree of hydration. The results were analyzed using theoretical models that represent the mortars as three-phase, interactive composites. The three phases are the matrix paste, the aggregate, and the thin interfacial transition zone between the two. The microstructure and properties of the conductive phases (the transition zone and the matrix paste) were determined by a micrometer-scale microstructural model, and were used in conjunction with random-walk algorithms and differential-effective medium theory to determine the overall mortar conductivities. The presence of the transition zone was not found to significantly affect the global electrical conductivity of the mortar. However, there were significant differences in conductivity between the transition zone and matrix pastes when examined on a local level. These differences were found to vary with hydration and were most significant when the degree of hydration was between 0.5 and 0.8.

I. Introduction

It has been generally shown that a thin, heterogeneous region of paste exists between the matrix cement paste and the aggregate surface in normal concrete or mortar. This region, commonly referred to as the interfacial transition zone (ITZ), is characterized by a higher concentration of calcium hydroxide crystals (CH^+) and an increased porosity relative to the matrix paste.[1–8] In the presence of low water/cement ratios and/or fine mineral admixtures (e.g., silica fume), the ITZ may be absent or difficult to detect.[9] Therefore, the ITZ is not necessarily an intrinsic feature of concrete, but will depend on factors such as the presence of admixtures, the type of mixing, the water/cement ratio, etc.[7] However, there is a preponderance of evidence that the ITZ exists in nearly all normal (w/c = 0.3–0.6) mix designs, without admixtures, such as those used in this study. The geometry of the cement grains and aggregates ensures that there will be inefficient packing of cement particles at the aggregate surfaces regardless of sample preparation, so that ITZ regions always potentially exist in concrete and mortar.

Because of the higher porosity in the ITZ, there is a concern that its presence might negatively impact the durability of cement-based materials by forming fast-conduction pathways through the material, allowing accelerated ingress and movement of aggressive species (e.g., Cl^-, CO_2, etc.).[10–12] As a result of this concern, there have been a number of studies that have attempted to quantify the transport properties of the ITZ.[13–20] The results of such experiments are difficult to understand because the presence of the aggregate necessitates at least three phases—aggregate, ITZ, and matrix paste. Extracting the influence of any one phase from the composite properties is therefore a difficult task. This is especially true when attempting to determine the influence of real transition zones, as opposed to the artificial ones created by casting cement paste against polished rock or glass surfaces.[7,21–23]

However, recent advances in the theoretical modeling of cement-based materials have made it possible to interpret transport experiments in terms of the influence of the ITZ in real mortars. This is especially important for the prediction of durability, as diffusion and electrical conduction are directly related by the Nernst–Einstein equation.[24] The discussion in this paper will focus on mortars exclusively. There are quantitative differences between mortars and concretes, but no qualitative differences. Electrical conductivity measurements made in parallel with microstructural modeling can provide a great deal of information concerning both the local and global effects of the ITZ on the conductivity of mortars.

II. Characteristics of the ITZ

The microstructure of mortars is more complex than neat paste.[8,25,26] This complexity is due to the formation of an ITZ between the matrix paste and aggregate surfaces. Although researchers are not in full agreement as to the mechanism of formation, it is generally accepted that the ITZ is the result of the inefficient packing of cement grains at the aggregate surface.[8] Thus, the near-aggregate surface region is deficient in hydration reactants, has a larger proportion of water, and therefore forms less space-filling product and more porosity. Additionally, the surfaces of the aggregate and the higher porosity promote the formation of a higher volume fraction of CH crystals, which tend to be more oriented than crystals in the bulk.[1,4] The reported thickness of the ITZ varies, but is typically in the range of 15 to 50 μm.[6,8,26] One reason for this large range of thicknesses is that there is no clear-cut transition from ITZ paste to matrix paste; hence the cut-off value is somewhat subjective. Generally, the ITZ can be considered to end when the porosity is within 10% of the bulk value. Modeling has shown that this thickness approximately scales as the median cement particle size.[27]

To date, two analytical tools have primarily been used to characterize the ITZ: scanning electron microscopy (SEM) and mercury intrusion porosimetry (MIP). SEM backscattered electron studies of polished sections in conjunction with computerized image analysis allow the porosity to be studied as a function of distance from the aggregate surface, as shown in Fig. 1.[5,6,28] These data show the porosity gradient as a function of distance from the aggregate, and an ITZ thickness of 15 to 30 μm, depending on how

N. J. Dudney—contributing editor

Manuscript No. 189695. Received December 14, 1998; approved August 26, 1999.
Supported by the National Science Foundation through the Science and Technology Center for Advanced Cement-Based Materials under Grant No. CHE-91-20002.
*Member, American Ceramic Society.
†Cement nomenclature will be used: C = CaO, H = H_2O, S = SiO_2.

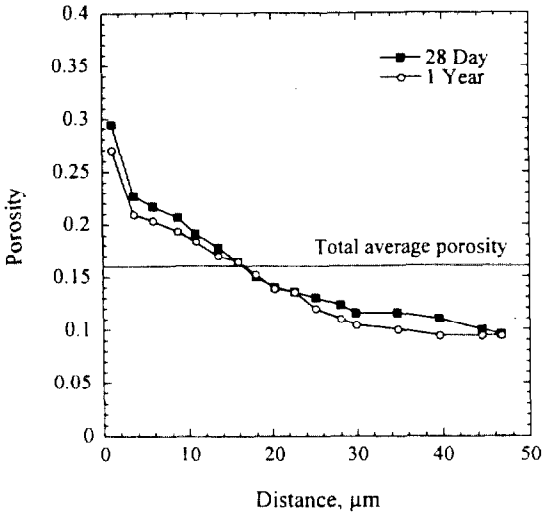

Fig. 1. Average porosity in the ITZ as a function of the distance from the aggregate surface for a concrete with water/cement = 0.4 (adapted from Scrivener[5]).

the cut-off is chosen.[5] There are two important details to note in this figure. First, the ITZ has a maximum porosity that is about 3 times higher than the matrix paste. Second, the presence of the ITZ affects the matrix paste by reducing its porosity compared with the nominal average porosity. Assuming the two have the same degree of hydration, this suggests the matrix paste has gained cement at the expense of the ITZ and thus has a reduced water/cement ratio.

MIP measures the overall porosity and approximate pore-size distribution of a material.[29] Mercury under pressure is injected into an evacuated sample, and the volume of mercury intruded at a given pressure is then related to the volume of pores of a diameter determined by the Washburn equation.[29] One of the shortcomings of this technique is that internal pore volumes will be attributed to the pore-neck diameters that connect them to the surface. Therefore, in mortars where the ITZ is not percolated through the sample (e.g., low volume fractions of sand), the volume of the ITZ pores will be wrongly assigned to pores of the matrix paste. However, once the ITZ is percolated through the sample, the ITZ and matrix paste pores can be differentiated. Mortars with depercolated and percolated interfacial zones are shown schematically in Figs. 2(a) and (b), respectively. In Fig. 2(a), the ITZ is not percolated across the sample, and the matrix paste needs to be infiltrated before the ITZ is intruded. Therefore, the larger ITZ pores will be assigned to the smaller bulk paste pore volume. However, in Fig. 2(b), the ITZ is percolated across the sample, and can be intruded before the matrix paste, so that the larger ITZ pores can be differentiated from the matrix pores.

This was demonstrated experimentally on mortars by Winslow *et al.*, whose data are shown in Fig. 3.[26] Their results show a noticeable jump, at larger pore diameters, between the intrusion curves for the samples containing volume fractions of sand less than 45% and greater than 49%. This leads to the conclusion that the ITZ has become percolated between these volume fractions of sand. Using these results in conjunction with a computer model of the mortar microstructure, Winslow *et al.* were able to show that the thickness of the ITZ was between 15 and 20 μm, agreeing well with the results of Scrivener *et al.*[5]

Although these results give important information concerning the general properties and microstructure of the ITZ and matrix pastes in mortar and concrete, they do little to enhance our understanding of the transport properties within the ITZ. Also, the sample preparation of these materials may disrupt the microstructure because the samples needed to be dried under vacuum before MIP characterization. The next section will detail the experimental and modeling results that do provide some insight into the influence of the ITZ on the transport properties of mortars on samples that were not dried.

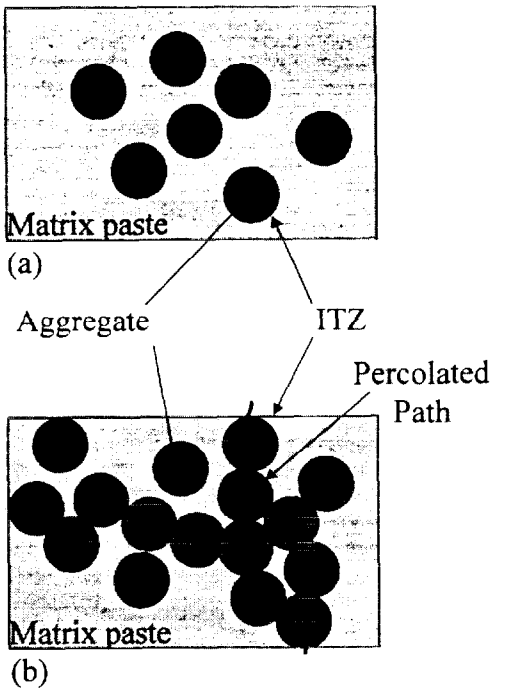

Fig. 2. Schematic of nonpercolated ITZ (a) and percolated ITZ (b) in cement mortars.

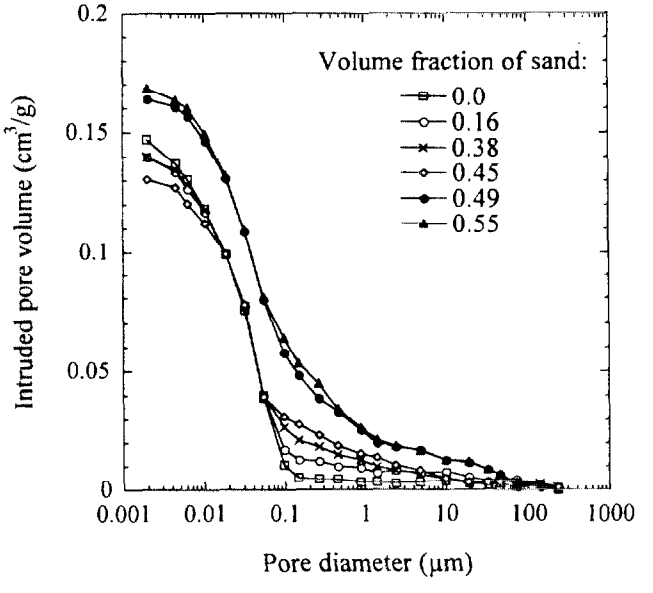

Fig. 3. MIP curves for neat portland cement mortars. Notice the significant gap in the intruded volume between the 45% and 49% sand volume fractions (adapted from Winslow *et al.*[26]).

III. Conductivity Studies of Mortars

(1) Experimental Procedure

The experimental portion of this study consisted of measuring the electrical properties of mortars with impedance spectroscopy (IS), an *in situ*, nondestructive technique.[30,31] IS separates the bulk and electrode responses of the material being measured, and uses low voltages (≈0.1 V/cm), so that the samples are not disrupted by the high fields sometimes necessary in dc measurements.[32] Although both capacitive and resistive information is measured with IS, only the dc resistance was used in this study. Measuring the ac response is still necessary, however, to be able to separate the electrode and bulk responses and get the true bulk conductivity. For the IS measurements, a Hewlett-Packard 4192A frequency

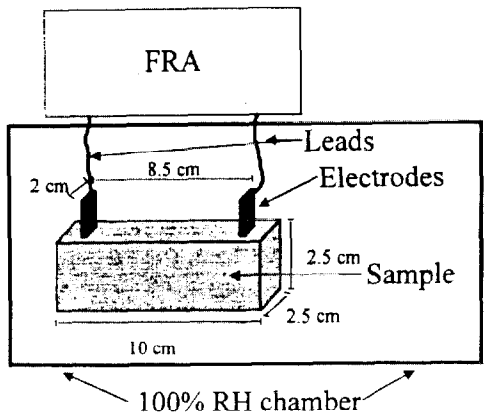

Fig. 4. Schematic of experimental setup indicating sample dimensions and electrode location.

response analyzer (FRA)[8] was used in the range of 5 Hz to 13 MHz, with 20 data points collected per frequency decade. The impedance spectra were corrected for parasitic lead effects.[33] The dc resistance of each sample was taken at the real impedance "cusp" between the bulk and electrode arcs.[31]

Mortar samples were made from a type I OPC (LaFarge) with a water/cement ratio of 0.40 and a silica sand conforming to ASTM C778. Sand volume fraction ($V_{f,sand}$) varied from 0.0 to 0.5, and conductivity was measured from time of mixing to 772 h of hydration time. The dry components were mixed in a Hobart planetary mixer for 1 min, after which water was added and the slurry was mixed for an additional 20 min (no superplasticizer was added). After mixing, the samples were cast into molds (25 mm × 25 mm × 100 mm) and vibrated under vacuum to reduce the volume of entrapped air. Flat stainless steel electrodes (19 mm × 40 mm, 19 mm × 25 mm embedded area) were embedded near the ends of the samples, with an interelectrode distance of 85 mm. No bleeding was observed in any of the samples. The specimens were stored and measured in a 100% relative humidity chamber at room temperature (see Fig. 4). Temperature increases during the early stages of hydration, although not quantified, were not significant after 24 h, when our first impedance measurements were made. To measure the degree of hydration, additional samples were prepared for loss-on-ignition (LOI) measurements. The samples were crushed, dried at 105°C, weighed, ignited at 1050°C for 90 min, and weighed again. LOI was calculated by dividing the mass loss by the ignited mass. The uncertainty in LOI measurements was estimated to be 0.01 g; the scatter at long hydration times is attributable to inadvertent differences in drying. The results indicate that the mortars and pastes hydrated at the same rate (see Fig. 5).

The measured mortar conductivities (σ_{mortar}) were normalized by the conductivity of a paste (σ_{paste}) with the same degree of hydration and water/cement ratio. (It is important to distinguish between the definition of paste and matrix paste. Matrix paste is one of three phases found in mortars, and resides between the aggregate particles (and ITZ paste see Fig. 2). "Paste," on the other hand, is defined as the single phase found in neat cement paste.) The raw conductivities for the mortars and paste at various ages are given in Table I and shown graphically in Fig. 6. Based on error estimates for cross-sectional area and interelectrode spacing, the uncertainty in measured conductivity is estimated at 5%. Because the mortars and pastes hydrate at the same rate, it is sufficient to normalize by pastes of the same age (see Fig. 5). In Fig. 6, the normalized values ($\sigma_{mortar}/\sigma_{paste}$), at a given degree of hydration, were plotted as a function of the volume fraction of sand

[8]Certain commercial equipment is identified in this paper to adequately specify the experimental procedure. In no case does such identification imply recommendation or endorsement by the National Institute of Standards and Technology, nor does it imply that the equipment used is necessarily the best available for the purpose.

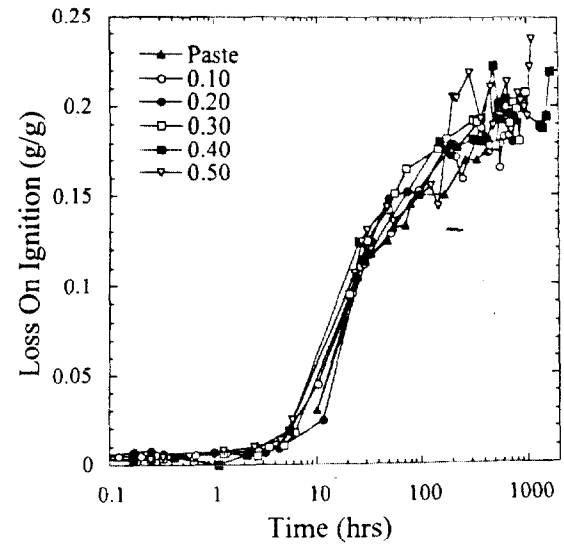

Fig. 5. Loss on ignition (g/g) versus hydration time for various mortars and paste used in this study. Mortars are labeled by their sand volume fraction.

for several degrees of hydration (hydration times), and were compared with the line of $(1 - V_{f,sand})^{3/2}$, which is the well-established Bruggeman–Hanai (B-H) law for the case of spherical, nonconductive particles in a conductive matrix.[34] This model assumes that the conductivity of the matrix is constant as nonconductive particles are added, so that the effect of the particles is to dilute the matrix and redirect conduction around themselves, making the conduction paths more tortuous. This by itself is a complicated many-body process. In the dilute limit of a low volume fraction of particles, it is known that the B-H law is exact. For general volume fractions of particles, this model has also been found to be accurate.[35] The derivation of this equation also seems to follow concrete microstructure more closely than other approximations, hence is to be preferred for this reason as well.[34,36] Also, there is no percolation threshold for the matrix or inclusions in this equation. The matrix is always connected, and the inclusions are always disconnected, as is the case in real concrete. Some of the other effective medium equations have different percolation thresholds. Therefore, if the matrix paste conductivity stays constant as more sand is added, and the effect of the ITZ on overall conductivity is negligible, then the experimental data should follow the model line. The data will go below the line if the ITZ regions have a negative effect on conductivity, and above the line if the ITZ regions have a positive effect on conductivity. If the presence of the ITZ regions also has an effect on the matrix, as was implied by Fig. 1, then a more careful analysis of the effect of the ITZ regions on mortar conductivity must be made, using a multiscale model, as is described next.

(2) Modeling

The mortar was modeled as a three-phase, multiscale interactive composite similar in nature to those previously considered by Garboczi and Schwartz.[37–39] A schematic of the model at the millimeter level is shown in Fig. 2. The model is considered interactive and multiscale because the volume fraction of aggregate (millimeter scale) and the thickness of the ITZ (micrometer scale) determine the final water/cement ratio of the matrix paste (micrometer scale). The median grain diameter of the cement used to make the pastes and mortars, 12 μm, was used as the thickness of the ITZ. The microstructure and properties of both the ITZ and matrix pastes are determined by a micrometer-scale microstructural model, and are used in conjunction with random-walk algorithms and differential-effective-medium theory to predict overall mortar conductivity.[37] The sand particles used in the model conformed to the particle size distribution of the sand used in the

Table I. Paste and Mortar Conductivities Measured by Impedance Spectroscopy at Various Times and Volume Fractions of Sand

	Conductivity ($(\Omega \cdot cm)^{-1}$)					
Time (h)	Paste	0.1	0.2	0.3	0.4	0.5
1	0.010 89	0.009 58	0.007 63	0.006 74	0.005 42	0.004 44
24	0.001 75	0.001 55	0.001 34	0.001 13	0.000 92	0.000 75
72	0.000 88	0.000 79	0.000 63	0.000 63	0.000 44	0.000 36
168	0.000 66	0.000 63	0.000 48	0.000 48	0.000 34	0.000 28
336	0.000 56	0.000 51	0.000 41	0.000 35	0.000 29	0.000 23
772	0.000 50	0.000 44	0.000 34	0.000 30	0.000 24	0.000 20

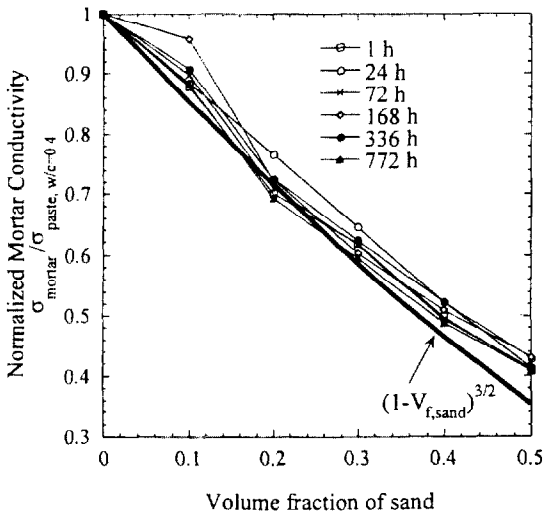

Fig. 6. Experimental mortar conductivities normalized by conductivity of paste (water/cement ratio = 0.4) versus volume fraction of sand.

experiments and were assumed to be spherical, nonconductive, and unreactive. Similar to the experimental results, the modeled results were normalized by the conductivity of a paste with the same water/cement ratio and degree of hydration. The results are shown in Fig. 7.

(3) Discussion

The agreement between modeling (Fig. 7) and experiment (Fig. 6) is reasonable, considering the complexity of the system under study. It is important to note that the models were not simply equations fitted to experimental data, but were derived from fundamental work, independent of the experimental data. In addition to modeling the overall conductivity, the models can also predict the properties of the constituent phases (see below).

The immediate and most important result of both the modeling and experimental data are that the ITZ does not seem to significantly enhance the overall electrical conductivity of the mortar (Figs. 6 and 7). This conclusion is based on a comparison of the normalized conductivities (mortar and paste, $\sigma_{mortar}/\sigma_{paste}$) with the $(1 - V_{f,sand})^{3/2}$ power law line. It would appear that the main effect of adding more sand is simply blocking and redirecting conductive flow, so that any effect of the ITZ is dominated by the effect of adding more aggregate.

The qualitative adherence to the $(1 - V_{f,sand})^{3/2}$ law requires additional discussion, however. Both modeling and other experimental work have demonstrated that when aggregate is added to cement paste, several things occur. First, the ITZ forms and increases in volume fraction in proportion to aggregate surface area (assuming a fixed thickness of ITZ). Second, since there is a lower amount of cement and greater amount of water in the ITZ and because the total amount of water and cement in the mortar is conserved, there must be a higher amount of cement and a lower amount of water in the matrix. This reduces the water/cement ratio of the matrix paste. Figure 8 shows the results of this redistribution of cement and water, using the multiscale model described above. The main utility of this model is the ability to carry out calculations like this. At the maximum amount of sand in the mortar, 50% by volume, the matrix water/cement ratio is reduced to 0.36 from a nominal value of 0.4, which will have a significant effect on the value of matrix paste conductivity. In concrete, which often has a volume fraction of aggregates of 60% or more, this effect will be even more pronounced. Therefore, as sand is added, the matrix paste conductivity is affected via the lowering of the water/cement ratio, as shown in Fig. 8. By closely examining the experimental data with the help of the multiscale model, the complex interplay between ITZ and matrix paste can be sorted out.

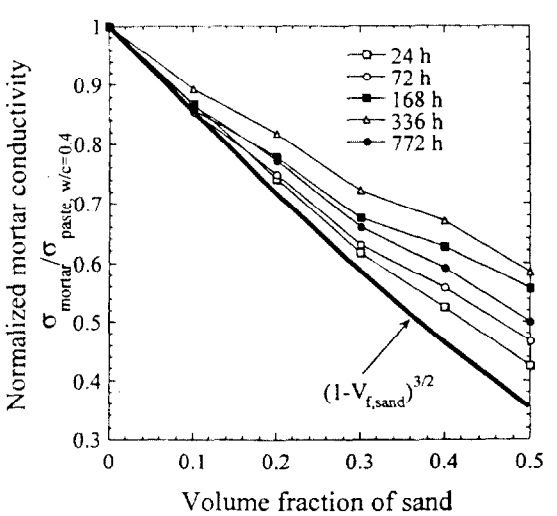

Fig. 7. Model mortar conductivities normalized by conductivity of a model paste (water/cement ratio = 0.4) versus volume fraction of sand.

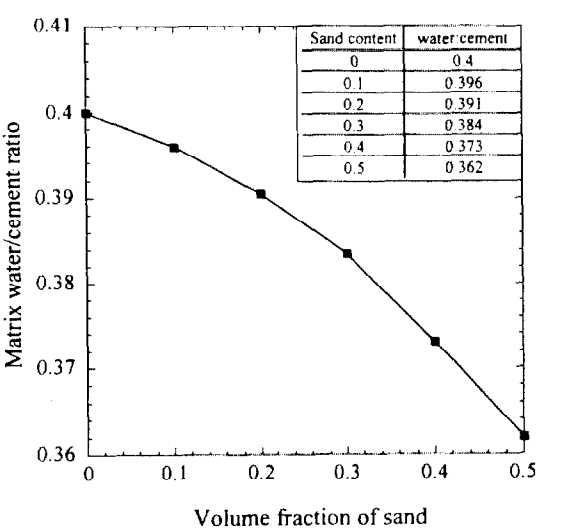

Fig. 8. Effect of volume fraction of aggregate on matrix water/cement ratio.

Some indication that complex interactive processes are taking place with time and with the addition of sand can be seen in the data in Figs. 6 and 7. For example, the normalized mortar conductivity ($\sigma_{mortar}/\sigma_{paste}$) starts near the B-H line, $(1 - V_{f,sand})^{3/2}$ at 1 h, deviates slightly above the line between 24 and 72 h, and approaches the line again subsequent to 336 h, for both the experimental and model data. Although this deviation is subtle, theoretical modeling can be used to provide insight as to what is happening to the paste contained in the ITZ and matrix. To quantify this, a factor, κ, will be defined: $\kappa = (\sigma_{mortar}/\sigma_{paste})/(1 - V_{f,sand})^{3/2}$. This is the normalized mortar conductivity divided by the value of the B-H law at a given volume fraction of sand. When κ is equal to 1, the normalized mortar conductivity ($\sigma_{mortar}/\sigma_{paste}$) lies exactly on the $(1 - V_{f,sand})^{3/2}$ line (the thick line in Figs. 6 and 7).

As mentioned previously, two things happen when aggregate is added to paste. First, the ITZ forms around the aggregate particles, increasing the local conductivity in the ITZ because of the higher porosity, which tends to increase the overall mortar conductivity. Second, the water/cement ratio of the matrix paste is reduced, which tends to lower the mortar conductivity. Although it is not possible to experimentally separate these two effects, the multiscale modeling results can be so used.

The κ values for the experimental mortar conductivity results are shown in Fig. 9 as a function of sand content (filled triangles). The open square symbols show the same value of κ for the experimental data, but with the mortar conductivity normalized by the matrix conductivity, as determined by the multiscale model. As the contrast between the ITZ and matrix conductivities develops and the ITZ volume fraction increases with the sand content, this modified κ value also increases. In contrast, the open circle symbols show how the ratio of the matrix paste conductivity to the nominal paste conductivity decreases when the sand content increases (from the multiscale model). Recall that the amount of sand governs the volume fraction of ITZ and therefore the reduction of the water/cement ratio of the matrix paste. The higher the ITZ volume fraction, the lower the water/cement ratio of the matrix paste. The net effect is a rough cancellation of positive (ITZ) and negative (matrix) contributions, to give the κ curve (triangles) shown in Fig. 9 (and Fig. 6).

The ratio of the conductivity of the ITZ and matrix pastes ($\sigma_{ITZ}/\sigma_{matrix}$) was predicted using the multiscale models.[37–39] This ratio, or contrast, is shown in Fig. 10 as a function of degree of hydration for a single volume fraction of sand ($V_{f,sand}$ = 20%). This plot shows that there is a marked dependence of this ratio on

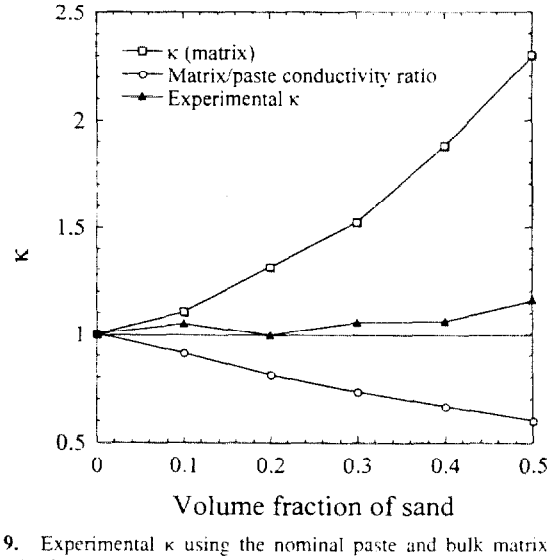

Fig. 9. Experimental κ using the nominal paste and bulk matrix paste normalizations, and the ratio of bulk matrix paste to nominal paste conductivity (see text for explanation) plotted versus volume fraction of sand. Note the opposite, but nearly equal conductivity contributions of the ITZ and matrix pastes. Data are for neat cement mortar at 72 h hydration (degree of hydration ≈0.63).

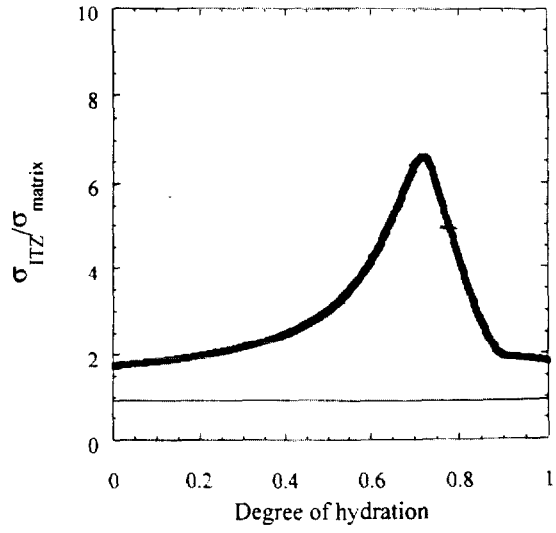

Fig. 10. Ratio of contrast between ITZ and matrix pastes determined by multiscale models (volume fraction of sand = 20%).

degree of hydration. There are several important features to note in the plot. First, the initial and final ratios are quite low ($\sigma_{ITZ}/\sigma_{matrix} \approx 2$). However, when the degree of hydration is in the range of 0.5 to 0.8 (equivalent to ~72 to 336 h of hydration at room temperature), the ratio shows a maximum value of approximately 7.

This behavior can be understood by examining the conductivity versus porosity curve for cement pastes, shown in Fig. 11. This curve was generated from an equation originally developed by Garboczi *et al.*,[24] has been verified experimentally,[40] and is part of the multiscale model.[37–39] The shape of the curve reflects the fact that in addition to the porosity decreasing with increasing hydration, there are also significant changes in the connectivity of the capillary pore structure. If it is assumed that the only difference between the ITZ and matrix paste is in initial porosity and that they track at the same rate along the same conductivity versus porosity curve, the general shape of the $\sigma_{ITZ}/\sigma_{matrix}$ curve can be explained. This is demonstrated graphically in Fig. 11 by the three sets of vertical and horizontal lines. The vertical lines differ by constant porosity, and the distances between the horizontal lines represent the corresponding differences in conductivities. Early and late in the hydration, the horizontal lines are spaced relatively closely, while near the middle of hydration, the horizontal lines have a significant gap, indicating there is a relatively large difference in

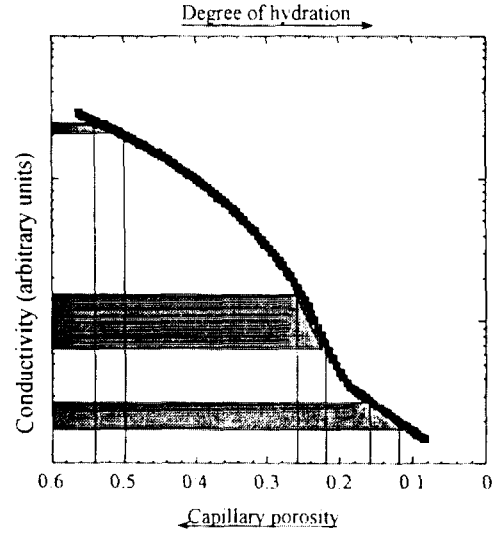

Fig. 11. Electrical conductivity of cement paste versus porosity determined by microstructural model and verified by experiment (after Ref. 24).

conductivity. This interpretation is borne out in both experiment and modeling by plotting $(\sigma_{mortar}/\sigma_{matrix})/(1 - V_{f,sand})^{3/2}$ versus the degree of hydration in Fig. 12. This term is similar to κ, except that it is normalized by the conductivity of the matrix, rather than of a paste of water/cement = 0.4. This reflects the increased conductivity of the ITZ as well as the reduced conductivity of the matrix as more aggregate is added. In Fig. 12, we can see that both the model and experimental results start at approximately unity, increase to a maximum value, then decrease again to a value close to unity. Recall that a value of 1 indicates the mortar behaves as if there was no influence of the ITZ.

Figures 10 and 12 clearly show that it is only during the middle stages of hydration that the ratio of ITZ to matrix paste conductivity is significant ($\approx$7). At a degree of hydration equal to $\approx$0.7 (equal to about 7 d of hydration at room temperature), the ratio is much smaller ($\approx$2), and the ITZ plays a relatively minor role in the overall mortar conductivity. Previous studies of a mortar assuming fixed conductivities for both matrix and ITZ paste[10,41] showed that a value of $\sigma_{ITZ}/\sigma_{matrix} \approx 6$ was necessary for the increased conductivity of the ITZ to overcome the decreased conductivity due to the insulating aggregate particles. Since the $\sigma_{ITZ}/\sigma_{matrix}$ ratio in the mortar in the present study only temporarily achieves that value and remains well below that value after a few hundred hours, the insulating effect of the aggregate wins out over the increased conductivity of the ITZ. The lowered conductivity of the matrix paste, due to the redistribution of cement and water, also contributes to negating the effect of the ITZ.

To overcome this redistribution effect, which was not considered in the previous studies mentioned,[10,41] it is estimated that a value for the $\sigma_{ITZ}/\sigma_{matrix}$ ratio on the order of 10–20 would be required to overcome the effect of the aggregate particles. Such a high value for the conductivity ratio is not realistic given the conductivity versus porosity dependence in Fig. 11. Since the highest value seen for $\sigma_{ITZ}/\sigma_{matrix}$ is less than 10, it is not likely that the ITZ will ever significantly enhance the conductivity of cement mortar.

It is interesting to compare the present results to some older experimental data by Whittington *et al.*[36] In this very careful paper, the conductivity of cement paste, mortar, and concrete was examined as a function of time and of aggregate volume fraction. The role of ITZ was not considered, and the ac frequency used to remove polarization effects appeared to be fixed, so there is no way of telling if the actual dc bulk resistance was measured or not. Also, only time was used as a variable, not degree of hydration. Keeping in mind these limitations, some comparisons can be made. For concrete, Whittington *et al.* found that conductivity, normalized by the conductivity of the cement paste from which it was made, approximately followed a power law in the quantity $(1 - V_{f,sand})$, but with a power of 1.2 rather than 1.5. They also found fluctuations in this ratio over time, but it is impossible to tell from their graphs whether this variation was similar to what was found in the present work. Aside from the emphasis on the ITZ in the present work, the ideas of Whittington *et al.*[36] have provided a basis for current thinking about concrete conductivity.

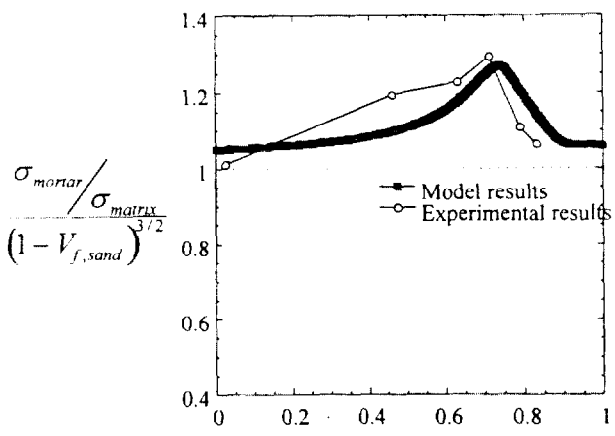

Fig. 12. Model and experimental $(\sigma_{mortar}/\sigma_{matrix})/(1 - V_{f,sand})^{3/2}$ factor versus degree of hydration for 20 vol% sand mortar.

(4) Permeability and the ITZ

It should be stressed that other transport parameters can be strongly affected, however, by the presence of the ITZ, properties like permeability and sorptivity, which are measures of fluid, rather than ionic, transport. Halamickova *et al.* have measured the hydraulic permeability of both mortars and pastes and found that the presence of aggregate particles significantly increased the coefficient of permeability in the mortar samples.[15] In fact, the hydraulic permeability of a mortar with 55 vol% of sand was 40 times higher than that of a paste with the same water/cement ratio and degree of hydration.

To show this graphically, the mortar permeabilities of Halamickova *et al.*[15] were normalized by a paste of the same water/cement ratio and degree of hydration and are shown in Fig. 13. These data are overlaid on a plot of the normalized mortar conductivity from the present study, all plotted as a function of sand content. Clearly the mortars show a marked increase in permeability, while the conductivity decreases as sand is added.

The contrast in conductivity between the ITZ and matrix paste conductivities in mortars and concrete is apparently not large enough for the ITZ to overcome the effect of the aggregate. This is because the conductivity is not a very strong function of the porosity, as seen in Fig. 11. However, fluid flow is different. The case of flow through a tube of circular cross section and radius r shows this clearly. For conduction, the electrical flow through such a tube is proportional to the total cross-sectional area r^2. In the same tube, fluid flow is proportional to r^4. Therefore, fluid flow, and thus permeability, are much more sensitive functions of pore size than is conductivity. Because of the larger pores and higher porosity in the ITZ compared with the matrix paste, the contrast between the permeabilities of the ITZ and matrix paste are thought to be much larger than for conductivity, perhaps 10–100 times as much. For such a large contrast, the positive effect of transport through the ITZ will dominate the negative effect of the blocking aggregate particles and the densified matrix paste. Thus, as in Fig. 13, permeability increases with additional sand content.

One way to approximately elucidate the effect of the ITZ on the permeability is to use the Katz–Thompson equation[42] and an MIP intrusion curve of a neat OPC paste and mortar.[26] The Katz–Thompson equation is

$$k_p = \frac{1}{226} d_c^2 \left(\frac{\sigma}{\sigma_0}\right) \quad (1)$$

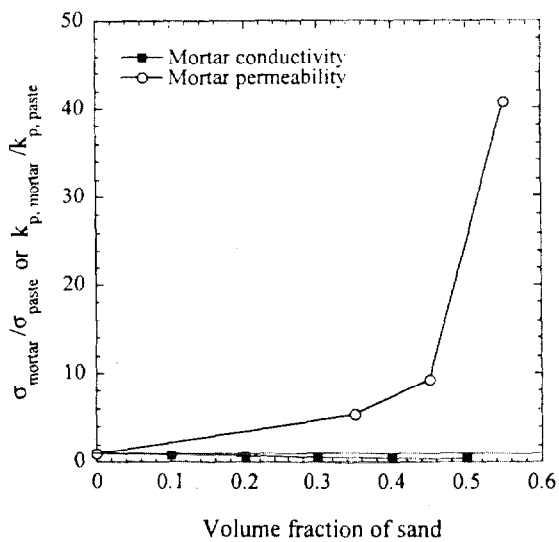

Fig. 13. Normalized permeability and conductivity data. Permeability data are adapted from Halamickova[15] (degree of hydration = 0.6), and conductivity data are from the present work (degree of hydration ~0.7).

where d_c is the critical pore diameter associated with the inflection point in the MIP intrusion curve, σ and σ_0 are the sample and pore fluid conductivities, respectively, and k_p is the hydraulic permeability.[42,43] The derivatives of two mercury intrusion curves are shown in Fig. 14. These curves are generated from two of the intrusion curves from Fig. 3 and indicate a bimodal distribution of pores for the mortar. The coarser pores are associated with the ITZ and the finer pores are assigned to the matrix cement paste. According to the d_c^2 term in the Katz–Thompson equation (assuming similar values for σ_0), the larger ITZ pores (d_c = 0.49 μm) will have a significantly higher permeability than the smaller matrix pores (d_c = 0.030 μm), and although the ITZ volume fraction is relatively low, it will have a significant influence on the overall permeability. It is also interesting to note that the paste portion of the two MIP curves indicates a slight shift to smaller pore diameters for the mortar. This is consistent with both the results of the model and of Scrivener *et al.*[6] which indicate that the water/cement ratio and thus the average pore size in the matrix are reduced when aggregate is present.

The applicability of the Katz–Thompson equation can be determined by looking at the critical pore diameters of an MIP intrusion curve for a paste and a mortar (e.g., Fig. 14). If the ITZ is percolated through the sample, the mortar can be roughly modeled as a parallel, three-phase composite, especially when the contrast between the ITZ and the matrix is large.[41] The volume fractions of the ITZ and matrix pastes are determined by the multiscale model shown in Fig. 7. The MIP intrusion data, as measured by Winslow *et al.*,[26] show a bimodal distribution of pores, with a critical pore diameter for the ITZ paste of 0.49 μm. The paste has a single pore-size distribution and a critical pore diameter of 0.030 μm. According to the Katz–Thompson equation, the two factors that influence the permeability are the normalized conductivity (σ/σ_0) and the critical pore diameter (d_c^2). It was demonstrated earlier that the conductivities of the ITZ and matrix are different by about a factor of 2 late in the hydration. Therefore, the ratio of the permeability of a mortar and a paste can be calculated by the following equation:

$$\frac{k_{p,ITZ}}{k_{p,paste}} = \frac{\sigma_{ITZ} \cdot d_{c,ITZ}^2}{\sigma_{paste} \cdot d_{c,paste}^2} = 2\left(\frac{0.49^2}{0.03^2}\right) = 534 \qquad (2)$$

According to this calculation, the ITZ is predicted to be ~500 times more permeable than the paste. However, not all the mortar is comprised of ITZ paste. Therefore, the result from Eq. (2) needs to be multiplied by the volume fraction of ITZ in the mortar (10% at 55 vol% sand, according to the model). Thus, assuming all the transport is through the ITZ, the mortar permeability is predicted to be about 50 times higher than that of a paste. This prediction can be compared with the experimental value in Fig. 13 of about 40. As can be seen in the figure, the agreement is reasonable. It should be noted that it is valid to use the MIP data by Winslow *et al.*[26] and the permeability data of Halamickova *et al.*[15] together for this comparison because the work of Halamickova was designed to follow the work of Winslow. (A similar comparison using the multiscale model can be found elsewhere.[41])

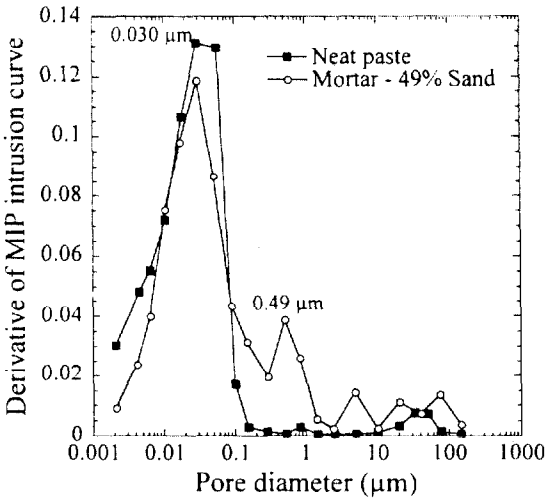

Fig. 14. The derivative of an MIP curve for a neat paste and a cement mortar showing approximate pore size distribution (adapted from Winslow[26]). Note the bimodal distribution of the mortar porosity.

It is also interesting to note in Fig. 13 that there seems to be a sharp upturn in the permeability of the mortar between 35 and 45 vol% sand. In agreement with the results of Winslow *et al.*,[26] this is an indication that the ITZ has become percolated. The conductivity does not show such an upturn because the contrast between the ITZ and matrix paste is too small. The upturn for the permeability is another piece of evidence for the higher contrast in permeabilities between ITZ and matrix paste. Further experimental and theoretical work is needed on the fluid flow properties of mortar and concrete as compared with cement paste.

IV. Conclusions

The electrical conductivity of cement pastes and mortars was measured as a function of volume fraction of sand and degree of hydration (hydration time) using impedance spectroscopy. These results were compared with theoretical models which were developed independently, but used experimental inputs such as the particle size distribution of the aggregate and the mean cement-grain diameter. The results indicate the following:

- The presence of the ITZ does not significantly enhance the overall conductivity of portland cement mortars. At low and high degrees of hydration, conductivity versus sand volume fraction follows the conventional Bruggeman–Hanai law, $(1 - V_{f,sand})^{3/2}$, when the conductivity of the mortar is normalized by the conductivity in the nominal paste matrix.
- There are two competing effects associated with the presence of aggregate that tend to counteract each other. The first is the creation of the porous, conductive ITZ in proportion to the aggregate surface area, and the second is the reduction of water/cement ratio in the matrix paste.
- The ratio of the ITZ and matrix paste conductivities ($\sigma_{ITZ}/\sigma_{matrix}$) starts out low (≈2) at early hydration, increases through a maximum (≈7), and then decreases to a low value (≈2). The maximum occurs at a degree of hydration between 0.5 and 0.8 (72 to 336 h) at room temperature.
- The contrast between the conductivities of the ITZ and matrix paste, $\sigma_{ITZ}/\sigma_{matrix}$, is low enough that the effect of the insulating aggregate dominates over the effect of the higher ITZ conductivity. As sand is added, the overall mortar conductivity always decreases at a fixed degree of hydration. This is not the case for other transport properties, e.g., fluid permeability.

References

[1]D. Bonen, "Calcium Hydroxide Deposition in the Near Interfacial Zone in Plain Concrete," *J. Am. Ceram. Soc.*, **77** [1] 193–96 (1994).

[2]B. D. Barnes, S. Diamond, and W. L. Dolch, "Micromorphology of the Interfacial Zone Around Aggregates in Portland Cement Mortar," *J. Am. Ceram. Soc.*, **62** [1–2] 21–24 (1978).

[3]D. Breton, A. Carles-Gibergues, G. Ballivy, and J. Grandet, "Contribution to the Formation Mechanism of the Transition Zone Between Rock-Cement Paste," *Cem. Concr. Res.*, **23** [2] 335–46 (1993).

[4]R. J. Detwiler, P. J. M. Monteiro, H. R. Wenk, and Z. Zhong, "Texture of Calcium Hydroxide Near the Cement Aggregate Interface," *Cem. Concr. Res.*, **18** [5] 823–29 (1988).

[5]K. L. Scrivener and K. M. Nemati, "The Percolation of Pore Space in the Cement Paste/Aggregate Interfacial Zone of Concrete," *Cem. Concr. Res.*, **26** [1] 35–40 (1996).

[6]K. L. Scrivener and E. Gartner, "Microstructural Gradients in Cement Paste Around Aggregate Particles," *Mater. Res. Soc. Symp. Proc.*, **114**, 77–85 (1988).

[7]A. W. Pope and H. M. Jennings, "The Influence of Mixing on the Microstructure of the Cement Paste/Aggregate Interfacial Zone and the Strength of Mortar" *J. Mater Sci.*, **27**, 6452–62 (1992).

[8]J. P. Ollivier, J. C. Maso, and B. Bourdette, "Interfacial Transition Zone in Concrete," *J. Adv. Cem. Based Mater.*, **2**, 30–38 (1995).

[9]M. G. Alexander, S. Mindess, S. Diamond, and L. Qu, "Properties of Paste–Rock Interfaces and Their Influence on Composite Behaviour," *Mater. Struct.*, **28**, 497–506 (1995).

[10]E. J. Garboczi, L. M. Schwartz, and D. P. Bentz, "Modeling the Influence of the Interfacial Zone on the DC Electrical Conductivity of Mortar," *J. Adv. Cem. Based Mater.*, **2**, 169–81 (1995).

[11]A. M. Vaysburd, "Durability of Lightweight Concrete Bridges in Severe Environments," *Concr. Int.*, 33–38 (1996).

[12]H. Uchikawa, "Mortar and Concrete from the Standpoints of Composition and Structure"; pp. 1–24 in Proceedings of the Engineering Foundation Conference on Advances in Cement Manufacture and Use (Potosi, MO). Engineering Foundation, New York, 1988.

[13]P. Xie, J. J. Beaudoin, and R. Brousseau, "Effect of Aggregate Size on Transition Zone Properties at the Portland Cement Paste Interface," *Cem. Concr. Res.*, **21** [6] 999–1005 (1991).

[14]P. Gu, P. Xie, and J. J. Beaudoin, "Microstructural Characterization of the Transition Zone in Cement Systems by Means of AC Impedance Spectroscopy," *Cem. Concr. Res.*, **23** [3] 581–91 (1993).

[15]P. Halamickova, R. J. Detwiler, D. P. Bentz, and E. J. Garboczi, "Water Permeability and Chloride Ion Diffusion in Portland Cement Paste Mortars: Relationship to Sand Content and Critical Pore Diameter," *Cem. Concr. Res.*, **25** [4] 790–802 (1995).

[16]A. Delagrave, J. P. Bigas, J. P. Ollivier, J. Marchand, and M. Pigeon, "Influence of the Interfacial Zone on the Chloride Diffusivity of Mortars," *J. Adv. Cem. Based Mater.*, **5**, 86–92 (1997).

[17]P. J. Tumidajski, "Electrical Conductivity of Portland Cement Mortars," *Cem. Concr. Res.*, **26** [4] 529–34 (1996).

[18]U. Costa, M. Facoetti, and F. Massazza, "Permeability of the Cement-Aggregate Interface: Influence of the Type of Cement, Water/Cement Ratio and Superplasticizer"; pp. 392–401 in *RILEM Symposium on Admixtures for Concrete: Improvement of Properties*. Chapman and Hall, Barcelona, Spain, 1990.

[19]X. Ping and J. J. Beaudoin, "Modification of Transition Zone Microstructure—Silica Fume Coating of Aggregate Surface," *Cem. Concr. Res.*, **22** [4] 597–604 (1992).

[20]X. Ping,, J. J. Beaudoin, and R. Brousseau, "Effect of Aggregate Size on Transition Zone Properties of the Portland Cement Paste Interface," *Cem. Concr. Res.*, **21** [6] 999–1005 (1991).

[21]P. J. M. Monteiro, J. C. Maso, and J. P. Ollivier, "The Aggregate Mortar Interface," *Cem. Concr. Res.*, **15** [6] 953–58 (1985).

[22]X. Ping, J. J. Beaudoin, and R. Brousseau, "Flat Aggregate–Portland Cement Paste Interfaces, II. Transition Zone Formation," *Cem. Concr. Res.*, **21** [5] 718–26 (1991).

[23]X. Ping, J. J. Beaudoin, and R. Brousseau, "Flat Aggregate-Portland Cement Paste Interfaces: I. Electrical Conductivity Models," *Cem. Concr. Res.*, **21** [4] 515–22 (1991).

[24]E. J. Garboczi and D. P. Bentz, "Computer Simulations of the Diffusivity of Cement-Based Materials," *J. Mater. Sci.*, **27**, 2083–92 (1992).

[25]P. Halamickova, "The Influence of Sand Content on the Microstructure Development and Transport Properties of Mortars," University of Toronto, Toronto, Canada, 1993.

[26]D. N. Winslow, M. D. Cohen, D. P. Bentz, K. A. Snyder, and A. J. Garboczi, "Percolation and Pore Structure in Mortars and Concrete," *Cem. Concr. Res.*, **24** [1] 25–37 (1994).

[27]D. P. Bentz, E. J. Garboczi, and P. E. Stutzman, "Computer Modelling of the Interfacial Zone in Concrete"; pp. 107–16 in *Interfaces in Cementitious Composites*. Edited by J. C. Maso. E&FN Spon, London, U.K., 1993.

[28]Y. Wang and S. Diamond, "An Approach to Quantitative Image Analysis for Cement Pastes," *Mater. Res. Soc. Symp. Proc.*, **370**, 23–32 (1995).

[29]D. N. Winslow, "The Validity of High Pressure Mercury Intrusion Porosimetry," *J. Colloid Interface Sci.*, **67** [1] 42–47 (1978).

[30]J. R. MacDonald, *Impedance Spectroscopy: Emphasizing Solid Materials and Systems*. Wiley Interscience, New York, 1987.

[31]B. J. Christensen, R. T. Coverdale, R. A. Olson, S. J. Ford, E. J. Garboczi, H. M. Jennings, and T. O. Mason, "Impedance Spectroscopy of Hydrating Cement-Based Materials: Measurement, Interpretation, and Application," *J. Am. Ceram. Soc.*, **77** [11] 2789–804 (1994).

[32]D. Sohn and T. O. Mason, "Electrically-Induced Microstructural Changes in Portland Cement Pastes," *J. Adv. Cem. Based Mater.*, **7**, 81–88 (1998).

[33]D. D. Edwards, J.-H. Hwang, S. J. Ford, and T. O. Mason, "Experimental Limitations in Impedance Spectroscopy: Part V—Apparatus Contributions and Corrections" *Solid State Ionics*, in press.

[34]D. S. McLachlan, M. Blaszkiewicz, and R. E. Newnham, "Electrical Resistivity of Composites," *J. Am. Ceram. Soc.*, **73** [8] 2187–203 (1990).

[35]R. E. De La Rue and C. W. Tobias, "On the Conductivity of Dispersions," *J. Electrochem. Soc.*, **106**, 827–33 (1959).

[36]H. W. Whittington, J. McCarter, and M. C. Forde, *Mag. Concr. Res.*, **33** [114] 48–60 (1981).

[37]E. J. Garboczi and D. P. Bentz, "Multi-Scale Analytical/Numerical Theory of the Diffusivity of Concrete," *J. Adv. Cem. Based Mater.*, **8**, 77–88 (1998).

[38]E. J. Garboczi and D. P. Bentz, "Analytical Formulas for Interfacial Transition Zone Properties," *J. Adv. Cem. Based Mater.*, **6**, 99–108 (1997).

[39]D. P. Bentz, E. J. Garboczi, and E. S. Lagergren, "Multi-Scale Modelling of Concrete Diffusivity: Identification of Significant Variables," *ASTM Cem. Concr. Aggregates*, **20**, 129–39 (1998).

[40]B. J. Christensen, T. O. Mason, H. M. Jennings, D. P. Bentz, and E. J. Garboczi, "Experimental and Computer Simulation Results for the Electrical Conductivity of Portland Cement Pastes," *Mater. Res. Soc. Symp. Proc.*, **245**, 259–64 (1992).

[41]L. M. Schwartz, E. J. Garboczi, and D. P. Bentz, "Interfacial Transport in Porous Media: Application to D.C Electrical Conductivity of Mortars," *J. Appl. Phys.*, **78**, 5898–908 (1995).

[42]A. J. Katz and A. H. Thompson, "Quantitative Prediction of Permeability in Porous Rock," *Phys. Rev. B*, **34** [11] 8179–81 (1986).

[43]A. J. Katz and A. H. Thompson, "Prediction of Rock Electrical Conductivity from Mercury Injection Measurements," *J. Geophys. Res.*, **92** [B1] 599–607 (1987). □